Semiconductor quantum dot mixture as a lossless negative dielectric constant optical material

Kevin J. Webb* and Alon Ludwig
School of Electrical and Computer Engineering, Purdue University, 465 Northwestern Avenue, West Lafayette, Indiana 47907-2035, USA

(Received 12 March 2008; revised manuscript received 9 August 2008; published 7 October 2008)

Prospects for a lossless negative dielectric constant material for optical devices are studied. Simulations show that, with sufficient gain, a mixture of two semiconductor quantum dots can produce an isotropic effective dielectric constant that is lossless and negative. Both analytical homogenizations based on the work of Maxwell Garnett and frequency-dependent dielectric constants from inversion of numerical computations of scattered fields are used to establish the dielectric constants of a mixture of gain and loss dots. Over length scales where homogenization is meaningful, this material could be used to achieve lossless "metal-insulator" optical waveguides and hence a small optical mode volume.

DOI: 10.1103/PhysRevB.78.153303 PACS number(s): 42.25.Bs, 78.20.Ci, 78.67.Hc

Achieving a negative dielectric constant at a frequency where the loss goes to zero, i.e., $\varepsilon(\omega_0)=\varepsilon'(\omega_0)+i\varepsilon''(\omega_0)$ with $\varepsilon''(\omega_0)=0$, is of fundamental importance in small-scale optics, which has come to be known as nanophotonics. A plasmon-polariton surface wave exists at a metal-insulator interface because of the negative dielectric constant for a mode with magnetic field parallel to the interface.[1,2] With two interacting surfaces, a metal-insulator-metal waveguide mode exists, and this propagates for arbitrarily small gaps. As the gap reduces, the wavelength reduces for a fixed free space wavelength. It is thus possible, in principle, to shrink the size of optical components using such mechanisms. Unfortunately, the loss increases as the waveguide-mode wavelength reduces, as measured per unit length.[1] Means to offset this loss would be of benefit in achieving small mode volumes and hence high-density optical elements and circuits.

Resonant states in semiconductor quantum wells provide a means of achieving a negative dielectric constant, provided that the dipole strength and oscillator density are adequate to offset the background,[3,4] as well as gain through optical or electrical pumping. We study a quantum dot (QD) mixture using both analytical and numerical homogenization methods and provide an estimate of the pumping energy to achieve a lossless negative dielectric constant at a single frequency.

Colloidal fabrication approaches that have been developed (for CdSe,[5,6] for example) have resulted in better than 5% variation in size.[7] Models typically employ an effective-mass approximation where the structure is assumed large relative to the crystal lattice dimension. In the case of a spherical QD under the strong confinement approximation, the wave function can be written as the product of the confined electron and hole functions, making an analytical solution possible, and the energies become the sum of the single-particle energies.[8,9] This simple model is assumed.

For a spherical potential well with infinite barriers at $r=R$, we assume the approximate exciton energy[8,9]

$$\epsilon = \epsilon_g + \frac{\hbar^2}{2m_{\mathrm{ex}}}k_{nl}^2 - \frac{1.8e^2}{4\pi\varepsilon_\infty\varepsilon_0 R}, \tag{1}$$

where ϵ_g is the intrinsic semiconductor band gap energy, the second term describes the kinetic energy of the exciton, and the third term gives the Coulomb potential of the electron and hole. Here it is assumed that the QD is in a background material of matched dielectric constant ε_∞, so there is no surface polarization screening charge; this is accounted for, approximately, in an homogenization calculation. In Eq. (1), ε_0 is the free space permittivity, $\hbar=h/(2\pi)$, with h being Planck's constant, and e is the electron charge. The exciton reduced mass is given by $m_{\mathrm{ex}}^{-1}=m_e^{*-1}+m_h^{*-1}$, with m_e^* being the effective mass of the electron and m_h^* the effective mass of the hole, and as $m_e^* \ll m_h^*$, a physical picture of a relatively immobile hole at the center of the QD applies. The k_{nl} are roots of $j_l(kR)=0$ with j_l being the spherical Bessel function of integer order l. The ground exciton state ($l=0$, $n=1$) gives $k_{10}=\pi/R$ in Eq. (1).

As the QD dimension is small relative to the wavelength of light, the Hamiltonian describing the interaction between the light field and the QD can be represented using the electric-dipole approximation,[10] which leads to a polarization and hence the QD dielectric constant $\varepsilon_{\mathrm{QD}}$. A density-matrix approach is used to determine the electric-dipole moment and hence $\varepsilon_{\mathrm{QD}}$.[11]

Consider the time-dependent wave function $|\Psi(t)\rangle = \Sigma_n C_n(t)|u_n\rangle$, where the normalized $|\Psi(t)\rangle$ gives $\Sigma_n|C_n(t)|^2 = 1$. Defining a density operator $\rho(t)=|\Psi(t)\rangle\langle\Psi(t)|$, the density matrix in the orthonormal set u_n is $\rho_{mn}(t)=\langle u_m|\rho(t)|u_n\rangle = C_n^*(t)C_m(t)$ with $\rho_{mn}=\rho_{nm}^*$.[10] The probability of the system being in state n is then ρ_{nn} averaged over a sufficient set of configurations, which is assumed. The equation of motion for the density matrix,[10] with phenomenological damping,[11] is

$$\frac{d\rho_{nm}}{dt} = \frac{-i}{\hbar}[H,\rho]_{nm} - \gamma_{nm}(\rho_{nm}-\rho_{nm}^{(0)}), \tag{2}$$

with commutator $[A,B]=AB-BA$, $\rho_{nm}^{(0)}$ the steady-state value [prior to application of the electric field $\mathbf{E}(t)$], and Hamiltonian $H=H_0+H(t)$ with $H(t)$ being the perturbation due to $\mathbf{E}(t)$.

The interaction Hamiltonian is $H(t)=-\boldsymbol{\mu}\cdot\mathbf{E}(t)$, and for the exciton, the dipole moment operator becomes $\boldsymbol{\mu}=e(\mathbf{r}_h-\mathbf{r}_e)$. The solution of Eq. (2), in the frequency domain with $\mathbf{E}(t)=\mathbf{E}\exp(-i\omega t)$, leads to a linear polarization

$\mathbf{P}(\omega)=N\langle\boldsymbol{\mu}(\omega)\rangle=\varepsilon_0\chi^{(1)}(\omega)\mathbf{E}(\omega)$ with oscillator density N and with the Cartesian components of the susceptibility matrix given by[11]

$$\chi^{(1)}_{ab}(\omega)=\frac{N}{\hbar\varepsilon_0}\sum_{nm}(\rho^{(0)}_{mm}-\rho^{(0)}_{nn})\frac{\mu^a_{mn}\mu^b_{nm}}{(\omega_{nm}-\omega)-i\gamma_{nm}}. \quad (3)$$

Noting that $\omega_{mn}=-\omega_{nm}$ and $\gamma_{nm}=\gamma_{mn}$, defining $P_q=\chi^{(1)}E_q$, and assuming a ground state $|g\rangle$,

$$\chi^{(1)}(\omega)=\frac{N}{3\hbar\varepsilon_0}\sum_n|\mu_{ng}|^2(\rho^{(0)}_{gg}-\rho^{(0)}_{nn})\times\left[\frac{1}{(\omega_{ng}-\omega)-i\gamma_{ng}}+\frac{1}{(\omega_{ng}+\omega)+i\gamma_{ng}}\right], \quad (4)$$

where the factor of 1/3 accounts for the average polarization mismatch. The oscillator strength is $f_{ng}=2m_{\mathrm{ex}}\omega_{ng}|\mu_{ng}|^2/(3\hbar e^2)$ and the Thomas-Reiche-Kuhn sum rule holds, giving $\Sigma_n f_{ng}=1$.[12] Consequently, Eq. (4), under the assumption that $\omega\sim\omega_{ng}$, leads to a QD susceptibility

$$\chi_{\mathrm{QD}}(\omega)=\frac{Ne^2}{\varepsilon_0 m_{\mathrm{ex}}}\sum_n f_{ng}\left[\frac{(\rho^{(0)}_{gg}-\rho^{(0)}_{ee})}{\omega^2_{ng}-\omega^2-i2\omega\gamma_{ng}}\right]. \quad (5)$$

Setting $N=8/V$ (where V is the QD volume) to account for degeneracy,[5,13] $m_{\mathrm{ex}}\approx m^*_e$, $(\rho^{(0)}_{gg}-\rho^{(0)}_{ee})=2\rho^{(0)}_{gg}-1$ (assuming a single exciton level), and with $\varepsilon=1+\chi$, Eq. (5) leads to

$$\varepsilon_{\mathrm{QD}}=\varepsilon_\infty+\frac{8e^2}{V\varepsilon_0 m^*_e}\left[\frac{(2\rho^{(0)}_{gg}-1)}{\omega^2_{\mathrm{ex}}-\omega^2-i2\omega\gamma}\right]. \quad (6)$$

For loss and gain, $\gamma>0$, and $\rho^{(0)}_{gg}>0.5$ provides a lossy resonance (absorption) and $\rho^{(0)}_{gg}<0.5$ gain. Neglecting thermally excited electrons, $\rho^{(0)}_{gg}=1$ for the lossy resonance and $\rho^{(0)}_{gg}=0$ for the gain resonance. We assume spherical QDs.

The homogenized dielectric constant $\varepsilon(\omega)$ for an ensemble of QDs having sufficiently low density (fill fraction) and dielectric constant can be described by the dielectric theory of Maxwell Garnett (MG).[14–17] For two quantum dot species, this becomes

$$\frac{\varepsilon(\omega)-\varepsilon_{\mathrm{bg}}(\omega)}{\varepsilon(\omega)+2\varepsilon_{\mathrm{bg}}(\omega)}=x_1\frac{\varepsilon_{\mathrm{QD1}}(\omega)-\varepsilon_{\mathrm{bg}}(\omega)}{\varepsilon_{\mathrm{QD1}}(\omega)+2\varepsilon_{\mathrm{bg}}(\omega)}+x_2\frac{\varepsilon_{\mathrm{QD2}}(\omega)-\varepsilon_{\mathrm{bg}}(\omega)}{\varepsilon_{\mathrm{QD2}}(\omega)+2\varepsilon_{\mathrm{bg}}(\omega)}=Q, \quad (7)$$

where x_j is the volume fraction of the jth QD species and $\varepsilon_{\mathrm{bg}}$ is the background dielectric constant. Equation (7) provides an approximate means to account for polarization charge from a mismatch between the QD and background dielectric constant. Solving Eq. (7) for ε gives

$$\varepsilon=\frac{\varepsilon_{\mathrm{bg}}(1+2Q)}{1-Q}. \quad (8)$$

We compare the MG results with a more rigorous homogenization approach based on a numerical calculation of scattering (S) parameter data, which we used for effective parameter extraction.[18] The numerical calculation of the S parameters was done using a full-wave vector finite element solver (HFSS). The QDs were represented by dielectric spheres with a homogeneous dielectric constant having a frequency dependence given by Eq. (6). We used periodic transverse boundary conditions to define a cell, resulting in two-dimensional periodicity normal to the incident-field direction (electric walls normal and magnetic walls parallel to the incident electric field, under the assumption of a quasistatic local field). The cell dimensions were determined from the QD size and volume fill fraction and, in our calculations, the largest cell dimension was less than $\lambda_{\mathrm{min}}/53$ with λ_{min} the smallest free space wavelength ($\lambda=2\pi c/\omega$, c being the speed of light in free space) over the frequency range we studied, making homogenization meaningful (even with the possible range of dielectric constants in the mixture). In the parameter extraction procedure, the effective-medium parameters were determined from the scattered fields parameterized by S parameters using

$$\varepsilon=\pm\frac{c}{\omega d}\sqrt{\frac{(1-S_{11})^2-S^2_{21}}{(1+S_{11})^2-S^2_{21}}}\cos^{-1}\left\{\frac{1}{2S_{21}}[1-(S^2_{11}-S^2_{21})]\right\}, \quad (9)$$

where S_{11} describes the electric field reflection and S_{21} the transmission through the slab, and d is the slab thickness. By studying the frequency-dependent solution and maintaining continuity in ε, the correct sign and branch of the arccosine function in Eq. (9) can be achieved. The convergence in ε was then studied as a function of the number of cells (in thickness) in order to arrive at the effective dielectric constant.

We considered CdSe QDs, and assumed that Eq. (1) gives the approximate exciton energy. Equation (6) was used to find the QD dielectric constant and then Eq. (8) to determine the homogenized dielectric constant for the QD mixture in a background. An ensemble of colloidally fabricated CdSe QDs have produced linewidths of $\hbar\gamma=0.04$ eV at room temperature and $\hbar\gamma=0.02$ eV at 10 K, limited by the variation in dimension of the QDs.[7] We used $m^*_e/m_0=0.1$, where m_0 is the electron rest mass, $\epsilon_g=1.74$ eV, and $\varepsilon_\infty=10.2$.

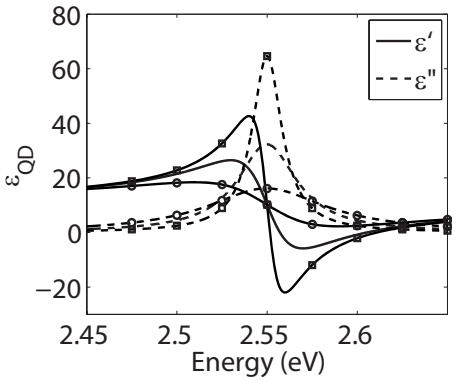

FIG. 1. Dielectric constant for a QD with $R=2$ nm and $\hbar\gamma=0.01$ (squares), 0.02 (no symbol), and 0.04 eV (circles).

Figure 1 gives $\varepsilon_{\mathrm{QD}}$ for several $\hbar\gamma$ values. Notice that $\hbar\gamma\leq 0.02$ is necessary to achieve a negative dielectric constant. The dependency of $\varepsilon_{\mathrm{QD}}$ on R is shown in Fig. 2. It is

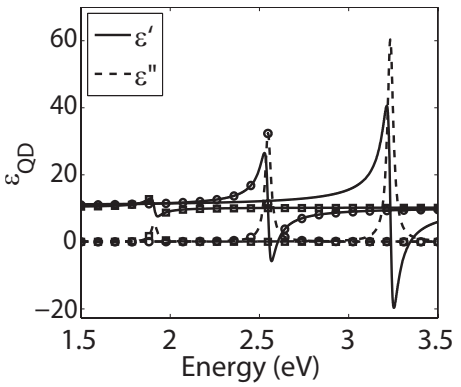

FIG. 2. Dielectric constant for a QD with varying R and $\hbar\gamma$=0.02 eV. R=1.5 (no symbol), 2 (circles), and 4 nm (squares).

evident that QDs with higher exciton energies and smaller R values offer more negative dielectric constants. This is because, within the assumption of an infinite barrier, the oscillator strength is inversely proportional to the volume of the QD. Consider now a mixture of QDs, described by Eq. (6), in a background ε_{bg} with an effective dielectric constant given by Eq. (8). Figure 3(a) shows the influence of variation in fill fraction x_1 (with x_2=0) and background dielectric constant ε_{bg}. Notice that the larger ε_{bg} produces a more negative ε. As one would expect, increasing x_1 produces a more negative ε. A rather optimistic $\hbar\gamma$=0.01 eV has been assumed. In Fig. 3(b), each of the plots of the effective dielectric constant from the upper panel that were obtained using the MG mixing rule is compared with the effective dielectric constant obtained using the full-wave parameter extraction procedure described earlier, with one QD per cell. In all the plots shown in Fig. 3(b), convergence of the effective dielectric constant was achieved using a slab of at most three QD cells (in thickness). It is evident from a comparison between the plots in Fig. 3(b) that, for the chosen parameters, the results of the MG mixing rule coincide with the results from the full-wave extraction procedure.

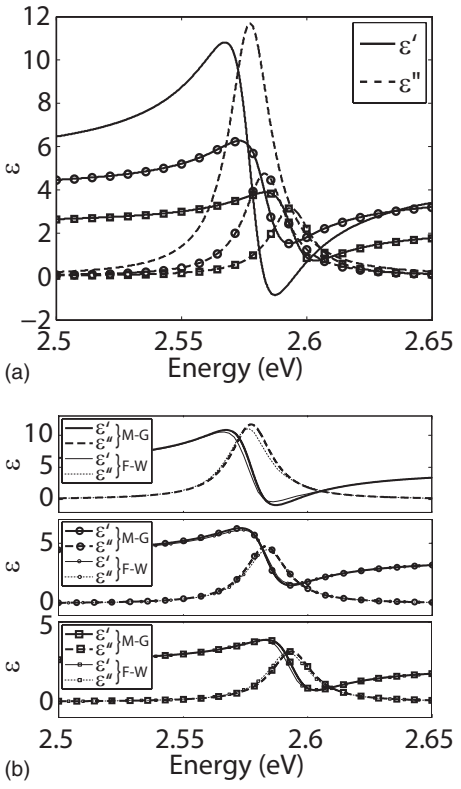

FIG. 3. (a) Effective dielectric constant for R=2 nm QDs with $\hbar\gamma$=0.01 eV and (i) ε_{bg}=3, x_1=0.4 (no symbol) and x_1=0.2 (circles) and (ii) ε_{bg}=1 and x_1=0.4 (squares). (b) Comparison of each of the plots in (a) that were obtained using the Maxwell Garnett mixing rule with results obtained via a full-wave effective-medium parameter extraction procedure.

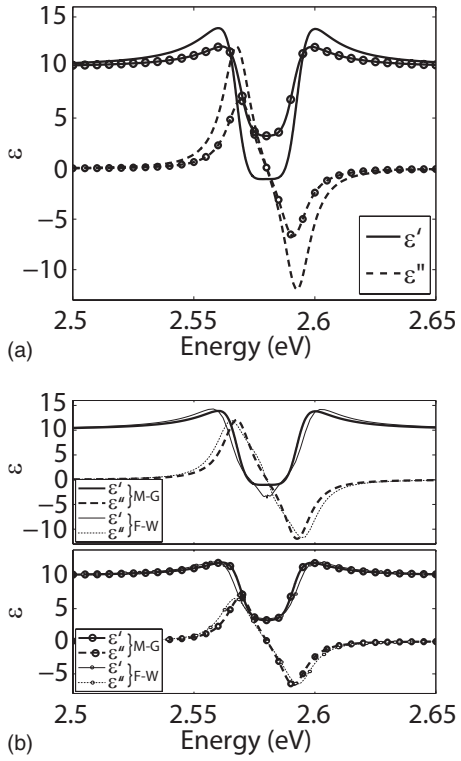

FIG. 4. (a) Effective dielectric constant for $R\approx$2 nm QDs with ε_{bg}=10 and $\hbar\delta$=0.06 eV with $x_1=x_2$=0.2 (no symbols) and $x_1=x_2$=0.1 (circles) assuming $\hbar\gamma$=0.007 eV. The gain is at the higher frequency. (b) Comparison of each of the plots in (a) that were obtained using the Maxwell Garnett mixing rule with those from a full-wave effective-medium parameter extraction procedure.

We require ε''=0 at some frequency in order to achieve lossless surface plasmons and hence lossless waveguide modes. To investigate prospects for obtaining isotropic material, consider distributions of two types of QDs, one providing an absorptive resonance and the other gain. The gain resonance is assumed to be at $\hbar\omega_{ex}+\hbar\delta$, where $\hbar\omega_{ex}$ is the loss resonance and $\hbar\delta$ is the energy difference achieved through a small reduction in dot size, which should satisfy $\hbar\delta>\hbar\gamma$. The gain is at the higher frequency, a condition that appears to be necessary to achieve a lossless plasmon operating condition.[19] Equal lossy and gain QD fill fractions are assumed, i.e., $x_1=x_2$. Figure 4(a) gives example results indicating that the conditions ε''=0 and $\varepsilon'<-1$ can be achieved with moderate to high fill fractions and a sufficiently small linewidth of $\hbar\gamma$=0.007 eV. In a manner similar to that of

Fig. 3, Fig. 4(b) shows a comparison between each of the plots of the effective dielectric constant in Fig. 4(a) obtained using the MG mixing rule and that obtained via the full-wave extraction procedure. In the electromagnetic simulation that was used for the extraction procedure, each cell was composed of four QDs with an absorptive resonance and four QDs with a gain resonance. Again, the validity of the parameters that were extracted was ascertained by their convergence with increasing number of cells (in thickness). While the effective dielectric constant for the lower filling factor ($x_1=x_2=0.1$) converged rapidly to values that are very close to those obtained by the MG mixing rule, the effective dielectric constant for the higher filling factor ($x_1=x_2=0.2$) demanded four cells to achieve convergence and converged to values that differ, to some extent, from the corresponding MG mixing rule values. The difference between the results obtained via the MG mixing rule and those obtained via the full-wave extraction procedure is due to the large filling factor ($x_{\text{total}}=x_1+x_2=0.4$) and the high contrast between the dielectric constant of the QDs and the background dielectric constant. When the effective ε' is minimal, in the middle of the plots, the contrast between both QDs and the background is high, leading to some difference between the MG mixing results and those obtained from the full-wave extraction procedure. Similar results can be obtained with a larger linewidth ($\hbar\gamma$) by increasing the filling factor.

Consider the (optical) pumping requirements to achieve the conditions $\varepsilon' \sim -1$ and $\varepsilon''=0$. Assume a QD excited-state lifetime of 10 ns (Ref. 20), which is long compared to available pump signals. Note that this lifetime can be substantially longer than the inverse of the linewidth [and the value $(2\gamma)^{-1}$ for an ensemble] under the assumption that the linewidth is limited by variation in QD size. Denote the pulse pumping rate as R_p photons/s and the pulse duration as T_p, and consider a pump volume V_p that has appropriate physical and optical characteristics. We assume fast pulse pumping where interlacing of the pumping and signal pulses allows the use of a two-level system with a high pumping pulse absorption rate. Thus, the pumping photon energy can be determined from the first energy level of the exciton. For each pump pulse, we require that all $8V_pN_{\text{QD}}$ excitons be lifted to the pumping energy level (including the factor of 8 for degeneracy), resulting in $R_pT_p \approx 8V_pN_{\text{QD}}$. With $R=2$ nm and $x_2=0.2$, the QD concentration is $N_{\text{QD}} \approx 6\times10^{18}$ cm^{-3}. This results in $R_pT_p/V_p=4.8\times10^{19}$ photons/(pulse cm^3). With a photon energy $\hbar\omega=2.55$ eV, we arrive at a rather substantial pump energy of 20 J/cm^3 per cycle. Small pump volumes are clearly necessary (1 mm^3 or smaller). To avoid ablation, the beam area could be increased while keeping the pump volume constant. Our analysis assumes that isolated QDs can be pumped, but the relatively high fill fraction and high pump rates could introduce electrical (Auger) interaction between dots that may present practical limitations.[21]

This study suggests that achieving a lossless isotropic metal at a single frequency is feasible. With sufficient oscillator strengths, it should be possible to reach a lossless frequency where the real part of the dielectric constant is negative (and less than -1). A comparison of the effective dielectric constant obtained via the MG mixing rule with the effective dielectric constant obtained from a full-wave parameter extraction procedure suggests that, while the MG mixing rule can give a good qualitative approximation to behavior of the QD mixture, numerical studies of the homogenized dielectric constant would be an appropriate prelude to experimental pursuits. The materials, in particular the background material, will be driven by the requirements for a negative dielectric constant from the mixture and thermal stability during optical pumping.

K.W. thanks L. Thylén for discussions that led to the idea presented in this Brief Report and Y. Fu and H. Ågren for subsequent collaborations, while on sabbatical at the Royal Institute of Technology, Stockholm. T. Feurer from the University of Bern provided valuable insight into possible implementations. This work was supported in part by the National Science Foundation (Contract No. 052442), the Army Research Office (Contract No. W911NF-07-1-0019), and the Department of Energy (Contract No. DE-FG52-06NA27505).

*webb@purdue.edu

[1] K. J. Webb and J. Li, Phys. Rev. B **73**, 033401 (2006).
[2] K. J. Webb and J. Li, Phys. Rev. B **72**, 201402(R) (2005).
[3] C. Delerue, G. Allan, and Y. M. Niquet, Phys. Rev. B **72**, 195316 (2005).
[4] Y. Fu, L. Thylén, and H. Ågren, Nano Lett. **8**, 1551 (2008).
[5] D. J. Norris, A. L. Efros, M. Rosen, and M. G. Bawendi, Phys. Rev. B **53**, 16347 (1996).
[6] X. Peng, J. Wickham, and A. P. Alivisatos, J. Am. Chem. Soc. **120**, 5343 (1998).
[7] C. B. Murray, C. R. Kagan, and M. G. Bawendi, Annu. Rev. Mater. Sci. **30**, 545 (2000).
[8] L. E. Brus, J. Chem. Phys. **80**, 4403 (1984).
[9] P. G. Bolcatto and C. R. Proetto, Phys. Rev. B **59**, 12487 (1999).
[10] J. J. Sakurai, *Modern Quantum Mechanics* (Benjamin/Cummings, Menlo Park, 1985).
[11] R. W. Boyd, *Nonlinear Optics* (Academic Press, San Diego, 1992).
[12] H. A. Bethe and E. E. Salpeter, *Quantum Mechanics of One- and Two-Electron Atoms* (Springer-Verlag, Berlin, 1957).
[13] A. Franceschetti, H. Fu, L. W. Wang, and A. Zunger, Phys. Rev. B **60**, 1819 (1999).
[14] J. C. M. Garnett, Philos. Trans. R. Soc. London, Ser. A **203**, 385 (1904).
[15] J. C. M. Garnett, Philos. Trans. R. Soc. London, Ser. A **205**, 237 (1906).
[16] R. W. Cohen, G. D. Cody, M. D. Coutts, and B. Abeles, Phys. Rev. B **8**, 3689 (1973).
[17] J. I. Gittleman and B. Abeles, Phys. Rev. B **15**, 3273 (1977).
[18] D. R. Smith, S. Schultz, P. Markoš, and C. M. Soukoulis, Phys. Rev. B **65**, 195104 (2002).
[19] K. J. Webb and L. Thylén, Opt. Lett. **33**, 747 (2008).
[20] C. R. Kagan, C. B. Murray, M. Nirmal, and M. G. Bawendi, Phys. Rev. Lett. **76**, 1517 (1996).
[21] C. Bonati, M. B. Mohamed, D. Tonti, G. Zgrablic, S. Haacke, F. van Mourik, and M. Chergui, Phys. Rev. B **71**, 205317 (2005).